Journal of Asian Concrete Federation
Vol. 11, No. 4, pp. 23-32, December 2025
ISSN 2465-7964/ eISSN 2465-7972
DOI http://dx.doi.org/10.18702/acf.2025.11.4.23

Technical Paper

Estimating Rebar Corrosion Distribution in Singly Reinforced Concrete with Stirrups using RBSM and Machine Learning

Keita Tateishi*, Tianyu Shao, Kohei Nagai

(Received: 29-Oct-2025; Revised: 02-Dec-2025; Accepted: 07-Dec-2025; Published online: 25-Dec-2025)

Abstract: Previous studies estimated internal corrosion distribution from surface cracks using Machine Learning and the Rigid Body Spring Model (RBSM). However, these models were limited to reinforced concrete (RC) without stirrups. Since most real structures contain stirrups, it is crucial to investigate whether the internal corrosion distribution can also be estimated for RC models with stirrups. So, in this study, we have investigated whether internal corrosion estimation is possible for singly reinforced RC models containing stirrups. A Convolutional Neural Network (CNN) was adopted, replacing the multilayer perceptron (MLP) used in prior study, to better learn the spatial patterns of corrosion. The CNN was trained using a dataset generated by RBSM simulations of a model without stirrups. As expected, the initial estimation accuracy for models with stirrups was low, as the training data lacked the confinement effect provided by stirrups. However, by iteration process proposed in previous research—an error correction loop where the crack width error is fed back to the network —it was demonstrated that the internal expansive strain distribution could be estimated with high accuracy. This validates the method's high flexibility and applicability for estimating corrosion in real structures.

Keywords: Machine Learning, Rigid Body Spring Model, corrosion, surface crack, stirrup, confinement

1. Introduction

In reinforced concrete (RC) structures, one of the primary causes of deterioration is the corrosion of reinforcing steel. The expansive pressure generated by the formation of corrosion products reduces the residual load-carrying capacity of RC members. Even when surface cracking is minimal or barely visible, corrosion-induced internal cracking can still cause the concrete cover to spall [1]. As corrosion progresses, the structural performance of RC members decreases, increasing the risk of spalling and failure. Therefore, evaluating the degree of rebar corrosion is of great importance for assessing the safety of RC structures.

In this context, various nondestructive techniques have been developed to indirectly assess internal corrosion using only surface-obtained information, such as the Half-Cell Potential (HCP) method [2], concrete resistivity [3], polarization resistance [4], and acoustic emission techniques [5][6]. However, these methods have notable limitations: for example, HCP measurements become difficult when the concrete or reinforcing bars are coated, and electrical connection to the rebar often requires partial removal of the concrete cover [7]. Moreover, these techniques generally provide only averaged estimates of corrosion level or rate, making it difficult to evaluate the detailed structural

*Corresponding author **Keita Tateishi,** *Graduate School of Engineering, Hokkaido University, Sapporo, Hokkaido 060−8628, Japan. E−mail: tateishi.keita.o3@elms.hokudai.ac.jp*
Tianyu Shao, *Department of Civil Engineering, The University of Tokyo, Tokyo 153−8505, Japan. E−mail: tianyu−shao@g.ecc.u−tokyo.ac.jp*
Kohei Nagai, *Graduate School of Engineering, Hokkaido University, Sapporo, Hokkaido 060−8628, Japan. E−mail: nagai325@eng.hokudai.ac.jp*

performance of RC members.

In recent years, new corrosion-estimation approaches have been proposed that aim to infer the internal corrosion distribution of reinforcement in RC members directly from surface crack widths using machine learning. Zhang et al. [8] generated a large synthetic dataset of surface crack widths and internal corrosion levels using three-dimensional finite element analysis combined with random-field modeling, and trained a neural network to estimate corrosion distribution from the resulting surface-cracking patterns. However, FEM cannot directly simulate localized cracking, and therefore has limitations in capturing the discrete nature of corrosion-induced cracking.

On the other hand, some studies adopted the three-dimensional Rigid Body Spring Model (3D-RBSM) for the same purpose. Since 3D-RBSM is a discrete analysis method capable of realistically simulating the complex propagation of corrosion-induced cracks, it has advantages over FEM for modeling localized cracking behavior. The validity of 3D-RBSM for corrosion analysis has been confirmed in previous studies, demonstrating that it can reliably reproduce both the initiation and propagation of corrosion-induced cracking [9][10][11][12].

Building on this capability, Kuntal et al. [13][14] integrated model predictive control (MPC) with RBSM and proposed an inverse-analysis framework (MPC-RBSM) that estimates internal expansive strain from observed surface crack widths. In MPC-RBSM, the surface cracks computed by RBSM are compared with the target cracks at each iteration, and the internal expansion strain is updated to minimize their difference. This iterative optimization enables the reconstructed corrosion distribution to gradually converge toward that implied by the observed cracking. However, prior studies have reported that the estimation accuracy of MPC-RBSM remains limited, partly because the expansion strain is optimized independently at each location without fully capturing the spatial correlation inherent in crack patterns. To address this issue, Shao et al. [15] later combined a multilayer perceptron (MLP) network with 3D-RBSM, allowing the network to learn the nonlinear mapping between surface crack widths and internal corrosion distributions using datasets generated by RBSM simulations. They demonstrated that this RBSM–MLP framework achieves high estimation accuracy for RC members with relatively simple reinforcement layouts, illustrating the potential benefits of incorporating machine learning into RBSM-based forward and inverse analysis.

Nevertheless, these machine-learning-based estimation frameworks have so far been limited to single-rebar RC configurations. In this study, the corrosion estimation model developed by Shao et al. [15] is applied to RC models with stirrups—previously excluded from the estimation targets—to examine whether accurate prediction is feasible. Since stirrups are present in most real RC structures and their presence fundamentally alters the internal stress state, the confinement effect on the concrete cover, and the propagation mechanism of corrosion-induced cracks, extending corrosion estimation to stirrup-confined members is essential for practical structural assessment. This study is the first to demonstrate that a machine-learning–based corrosion estimation model trained on a no-stirrup RC dataset can be successfully extended to RC members with stirrups through the proposed iteration-based error-correction process.

2. Numerical model

2.1 Rigid body spring model (RBSM)

RBSM was originally proposed by Kawai et al. [16] in 1978 as a discrete analytical approach and was later extended to three-dimensional mesoscale analysis by Nagai et al. [17]. In the 3D-RBSM, as illustrated in Fig. 1, each rigid element possesses six degrees of freedom—three translational and three rotational—and is connected to adjacent elements through one normal spring and three shear springs to simulate stress transfer between elements.

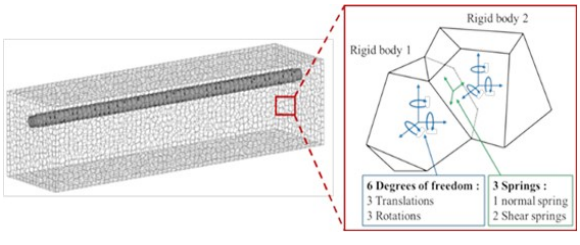

Fig. 1. 3D model with Voronoi discretization and spring details

2.2 Constitutive model

The constitutive models employed in this study are illustrated in Figs. 2a–d and Eqs. 1–5. The model consists of bi-linear softening behavior in concrete tension, elasto-plastic shear behavior of concrete, elasto-plastic steel with strain hardening, and elastic shear response. The interface between concrete and steel is modeled using the same springs as those between concrete elements but with half the tensile strength.

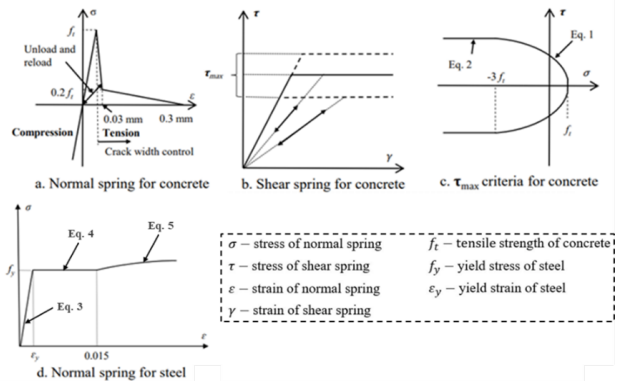

Fig. 2. Constitutive models of springs for concrete and steel

2.3. Corrosion expansion model

As shown in Fig. 3, the corrosion of reinforcing steel was simulated using the Corrosion Expansion Model (CEM), in which expansion strain was incrementally introduced step by step into the normal springs located at the interfaces between steel and concrete elements.

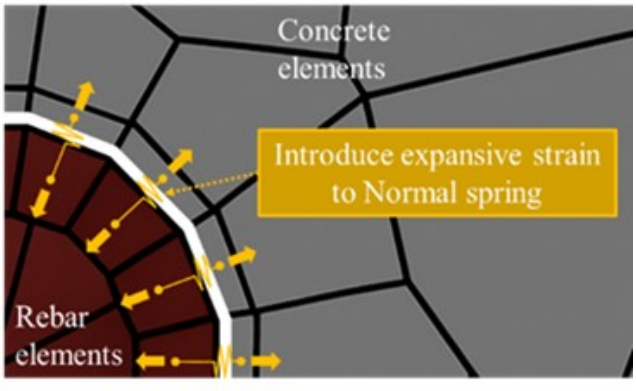

Fig. 3. Corrosion expansion model

$$\tau_{max} = \pm\left(1.6f_t^2(-\sigma + f_t)^{0.4} + 0.15f_t\right) \quad for \quad -3f_t \le \sigma \le f_t \quad (1)$$

$$\tau_{max} = \pm\left(1.6f_t^2(4f_t)^{0.4} + 0.15f_t\right) \quad for \quad \sigma \le -3f_t \quad (2)$$

$$\sigma_s = E_s\varepsilon_s \quad for \quad \varepsilon_s \le \varepsilon_y \quad (3)$$

$$\sigma_s = f_y \quad for \quad \varepsilon_y \le \varepsilon_s \le \varepsilon_{sh} \quad (4)$$

$$\sigma_s = f_y + \left(1 - e^{\frac{\varepsilon_{sh}-\varepsilon_s}{k}}(1.01f_u - f_y)\right) \quad for \quad \varepsilon_{sh} \le \varepsilon_s \quad (5)$$

3. Framework of RBSM–neural network system

The estimation framework of this study is illustrated in Fig. 4. In Phase I, datasets are generated, and a corrosion estimation model is trained using the constructed datasets. In Phase II, the trained model from Phase I is applied to estimate the internal corrosion distribution. The crack width distribution of the target structure is input into the trained model to obtain the initial estimation of the internal corrosion. The estimated corrosion distribution is then used as input data for corrosion analysis by the RBSM, from which the corresponding surface crack width distribution is computed. If differences are found between the target and estimated crack width distributions, the crack width error is fed back into the network, and the estimated corrosion distribution is optimized through an iteration process. This iterative process continues until the difference between the target and estimated crack width distributions becomes sufficiently small, after which Phase III begins. In Phase III, the final estimated corrosion distribution is used as input for an RBSM-based corrosion analysis to calculate the internal stress and cracking conditions, from which the mechanical performance of the target RC structure is evaluated.

The iteration process not only contributes to minimizing estimation error but also improves the flexibility of the estimation framework. Shao et al. [15] demonstrated that even when the cover thickness of the main reinforcing bars differs between the training and target RC models, several iterations can significantly enhance the estimation accuracy. Therefore, by incorporating the iteration process, the proposed model can accurately estimate corrosion distributions for RC structures with different cover thicknesses and rebar arrangements from those used in the training phase, thereby improving the robustness and generalization capability of the estimation framework.

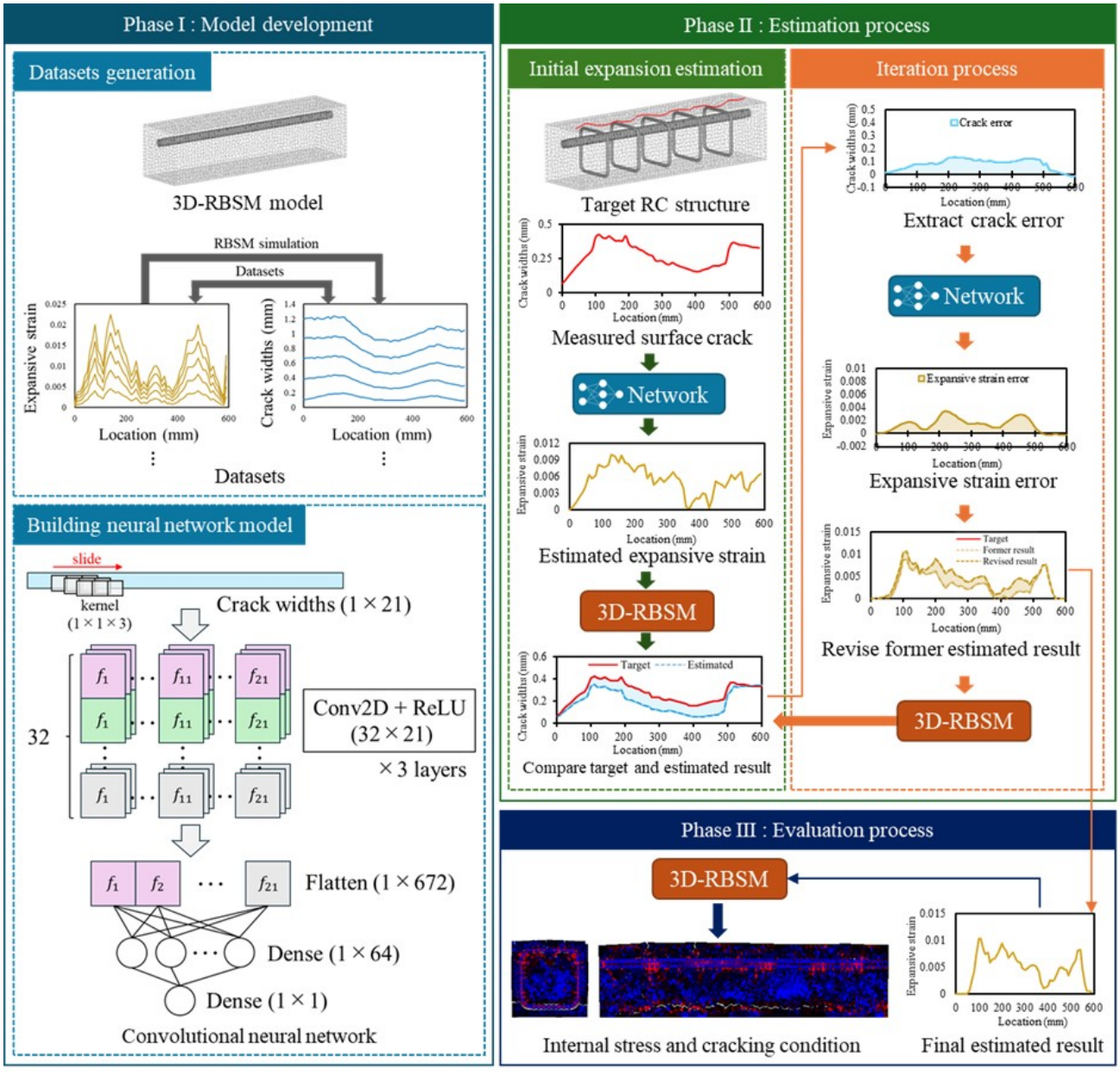

Fig. 4. Framework of RBSM-neural network estimation system

Next, in the tidal and splash zone, contrary to the results for the submerged zone, shrinkage behavior was observed for all parameters, and a similar decreasing trend was observed for the rate of mass change. This is thought to be largely due to the addition of dry conditions in the tidal and splash zone. As for the trend of each parameter, EX50S with a restrained rebar ratio of 0.5% tended to show larger shrinkage strain and mass loss rate due to drying, similar to PL50. However, EX50M and EX50L, which have constrained rebar ratios of 1.0% and 2.0%, showed smaller shrinkage strain and mass loss rate due to drying compared to PL50. This may be due to the effect of restraint by the steel bars. As the ratio of restrained steel bars increased, the shrinkage restraint stress increased and the drying shrinkage strain decreased. In this paper, the effect of the ratio of restrained steel bars and the shrinkage reduction effect of the expansion material were also confirmed in EX50M and EX50L, where the effect of restraint was relatively large.

4. Neural network training

4.1 Database for network

The construction of a machine learning–based prediction model requires a large amount of training data. Although it is most desirable to obtain such datasets experimentally, this approach is often constrained by cost and time limitations. Therefore, in this study, an alternative approach was adopted in which corrosion simulations using the 3D-RBSM were conducted to generate the datasets required for model training.

4.1.1 Model description

Fig. 5 and Fig. 6 show the RC model (S-0) prepared for dataset generation in this study. The mesh sizes of the concrete and steel elements were set to 10 mm and 5 mm, respectively. The material properties of the reinforcing steel and concrete used in the model are listed in Table 1. Corrosion-induced expansion strain was applied to the entire length of the main reinforcing bars at 10 mm intervals. Crack width data were calculated as the relative displacement between adjacent elements located on both sides of a crack at 10 mm intervals, with a gauge length of 70 mm. In actual RC structures, the stirrups on the cover concrete side are generally corroded together with the main reinforcing bars; however, for simplicity, corrosion was applied only to the main bars in this study.

Table 1. Material properties

	Elastic modulus (GPa)	Poisson's ratio	Tensile/ yielding strength (MPa)	Compressive strength (MPa)
Concrete	35	0.18	3.0	30
Steel	200	0.25	450	/

4.12 Data preparation for training

Corrosion analyses were performed by applying various corrosion distributions, including geometric shapes (e.g., triangular or linear patterns) and random shapes. A total of 50 simulations, each consisting of 50 analysis steps, were conducted—18 cases with geometric shapes and 32 cases with random shapes—resulting in the generation of 2,500 datasets ("Datasets generation" in Phase I of Fig. 4).

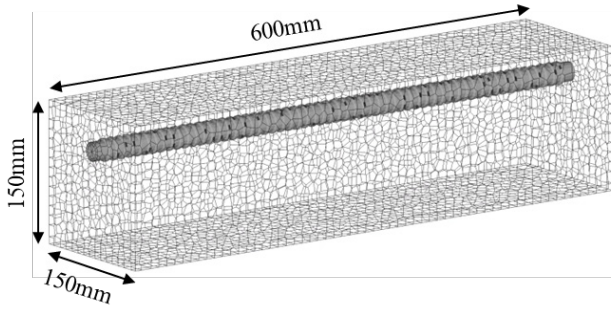

Fig. 5. Overview of the model

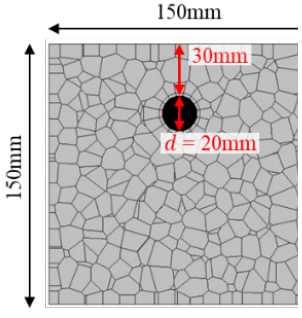

Fig. 6. Cross section of the model

4.2 Neural network structure

In previous studies, a multilayer perceptron (MLP) network was employed for corrosion estimation. Although the MLP has a simple and versatile architecture, its ability to capture spatial relationships is limited. To analyze RC structures with multiple longitudinal bars, a neural network capable of learning spatial correlations was therefore required. Hence, a convolutional neural network (CNN) was adopted. In this study, the input to the CNN is the surface crack width distribution, and the output (training label) is the internal expansive strain distribution imposed in the RBSM simulations as the corrosion-induced expansion. Thus, the CNN is trained to learn the mapping from surface cracks to internal corrosion.

A CNN is widely used in image recognition to detect spatial features by sliding small filters (kernels) over two-dimensional inputs. It typically consists of convolutional, pooling, and fully connected layers,

where the first extracts local features, the second reduces dimensionality, and the last integrates higher-level features for prediction. In this study, the pooling layer was omitted to preserve the one-to-one positional correspondence between each crack-width input point and the corrosion value predicted at the same location. The window size, determining the number of crack width inputs, was set to 21 points (10 on each side of the target point). The overall CNN architecture is shown in Fig. 4 ("Building neural network model" in Phase I).

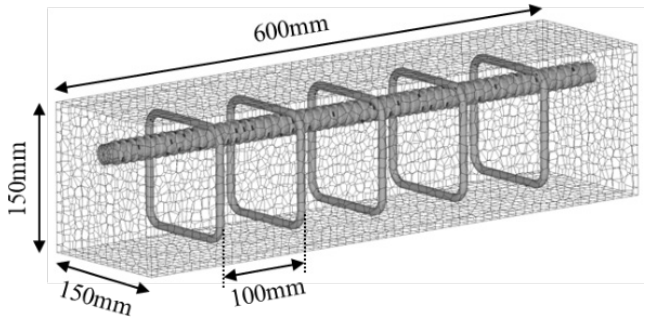

Fig. 7. Overview of S-5

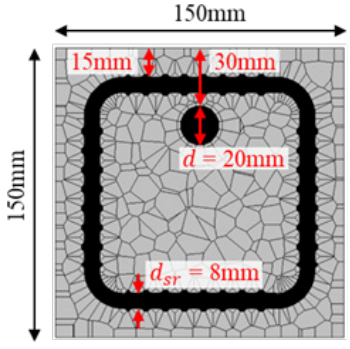

Fig. 8. Cross section at stirrup position

5. Estimation process of singly reinforced concrete with stirrups

5.1 Model description

Fig. 7 presents an overview of the RC model with five stirrups (S-5) used as the target for corrosion estimation, and Fig. 8 shows the cross-sectional view at the stirrup positions. The spacing between the stirrups was uniformly set to 100 mm. The diameter and cover thickness of the main reinforcing bars in S-5 are identical to those of the RC model described in Section 4.1.1 (S-0). Besides, the input material properties of concrete and reinforcements are presented in Table 1.

5.2 Estimation results

Figs. 9, 10, and 11 summarize the estimation results obtained in this study, with the upper part of each figure showing the results for the no-stirrup model (S-0) and the lower part showing the results for the stirrup-containing model (S-5).

Fig. 9 presents the predicted crack widths and expansive strains before and after the iteration process. "target" represents the ground truth data, while "0 iteration" denotes the initial estimation result (before any error correction through the iteration process). "1 iteration" and "2 iterations" indicate the estimation results after one and two iterations of error correction, respectively.

5.2.1 An example of estimation results for the no–stirrup model (S–0)

For the S-0 model (upper part of Fig. 9), the CNN already provides highly accurate predictions for the S-0 model from the initial (0 iteration) output, and the subsequent iterations further reduce the small remaining errors. In this process, the corrosion distribution estimated by the CNN is first input into the RBSM simulation to compute the corresponding surface crack width. The difference between this simulated crack-width distribution and the real crack-width distribution is then visualized in Fig. 9, and this error distribution is fed back into the network to perform the iterative error-correction process illustrated in Fig. 4. The upper part of Fig. 10 shows that the surface crack patterns of the S-0 model are reproduced almost perfectly after two iterations, reflecting the high accuracy observed in Fig. 9. Similarly, the upper part of Fig. 11 confirms that the internal stress and cracking conditions for S-0 are accurately reproduced across all cross-sections.

These consistent results verify that the CNN exhibits excellent baseline performance for the configuration used in training.

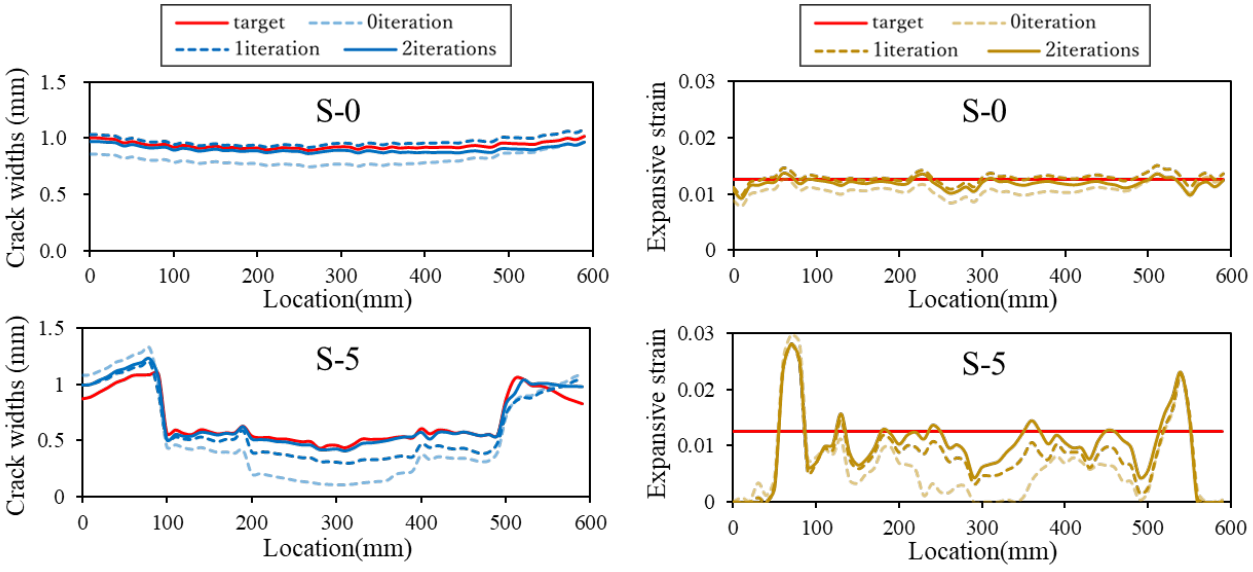

Fig. 9. One example of estimation result (left: crack widths, right: expansive strain)

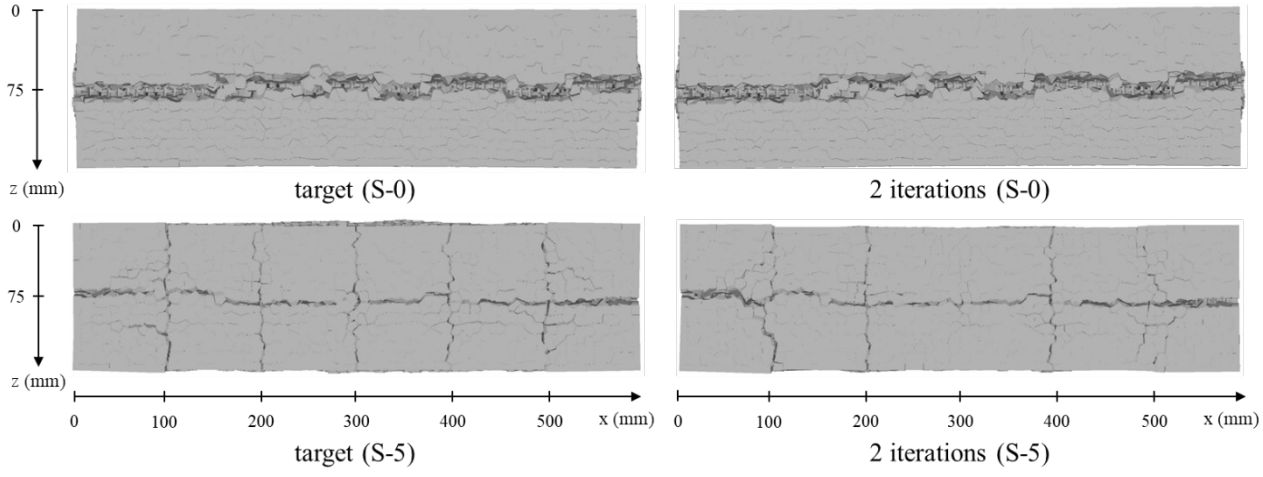

Fig. 10. Surface crack patterns of target and 2 iterations (deformation magnified 10 times)

5.2.2 An example of estimation results for the stirrup–containing model (S–5)

For the S-5 model, the lower part of Fig. 9 shows that the initial estimation (0 iteration) contains significant discrepancies from the target crack width distribution because the training dataset did not include the confinement effect of stirrups. However, as the iteration process proceeds (1 and 2 iterations), the estimation accuracy progressively improves. After two iterations, the predicted crack width distribution closely matches the target, and the mean absolute errors (MAEs) of the crack width and expansive strain decrease to approximately 0.040 mm and 0.0051, respectively. As discussed in Section 3, these improvements

demonstrate that the iteration process enhances the model's ability to estimate corrosion for

RC configurations not included in the training data, thereby highlighting the flexibility and generalizability of the proposed approach.

The lower part of Fig. 10 shows that the overall surface crack pattern of the S-5 model is also reasonably well captured after two iterations, although the crack extending in the z-direction at x = 300 mm is not fully reproduced. The lower part of Fig. 11 demonstrates that the internal stress state and cracking

conditions are similarly well reproduced, except for some discrepancies at the x = 300 mm section.

Overall, the results confirm that high-accuracy estimation is achieved for the S-5 model after applying the iteration process.

Taken together, the results for both the no-stirrup model (S-0) and the stirrup-containing model (S-5) confirm that the newly adopted CNN successfully estimated the internal corrosion distribution regardless of the presence of stirrups. While previous studies employed an MLP network, the CNN demonstrated a markedly higher capability in learning spatial patterns, achieving high prediction accuracy in both cases. These findings indicate that the proposed approach has strong potential for application to more complex estimation problems, including RC members with multi-rebar configurations and more intricate stress states.

6. Conclusions

1)By applying the error-correction technique, the estimation model trained on the relationship between internal corrosion and surface cracking of a single-rebar RC model without stirrups successfully estimated the internal expansion strain of a single-rebar RC model with stirrups with a practical MAE of 0.0010–0.0020.

2)While previous studies employed a MLP network as the neural network architecture, this study adopted a CNN, which is more suitable for learning spatial patterns, to estimate the corrosion distribution. The prediction results exhibited high

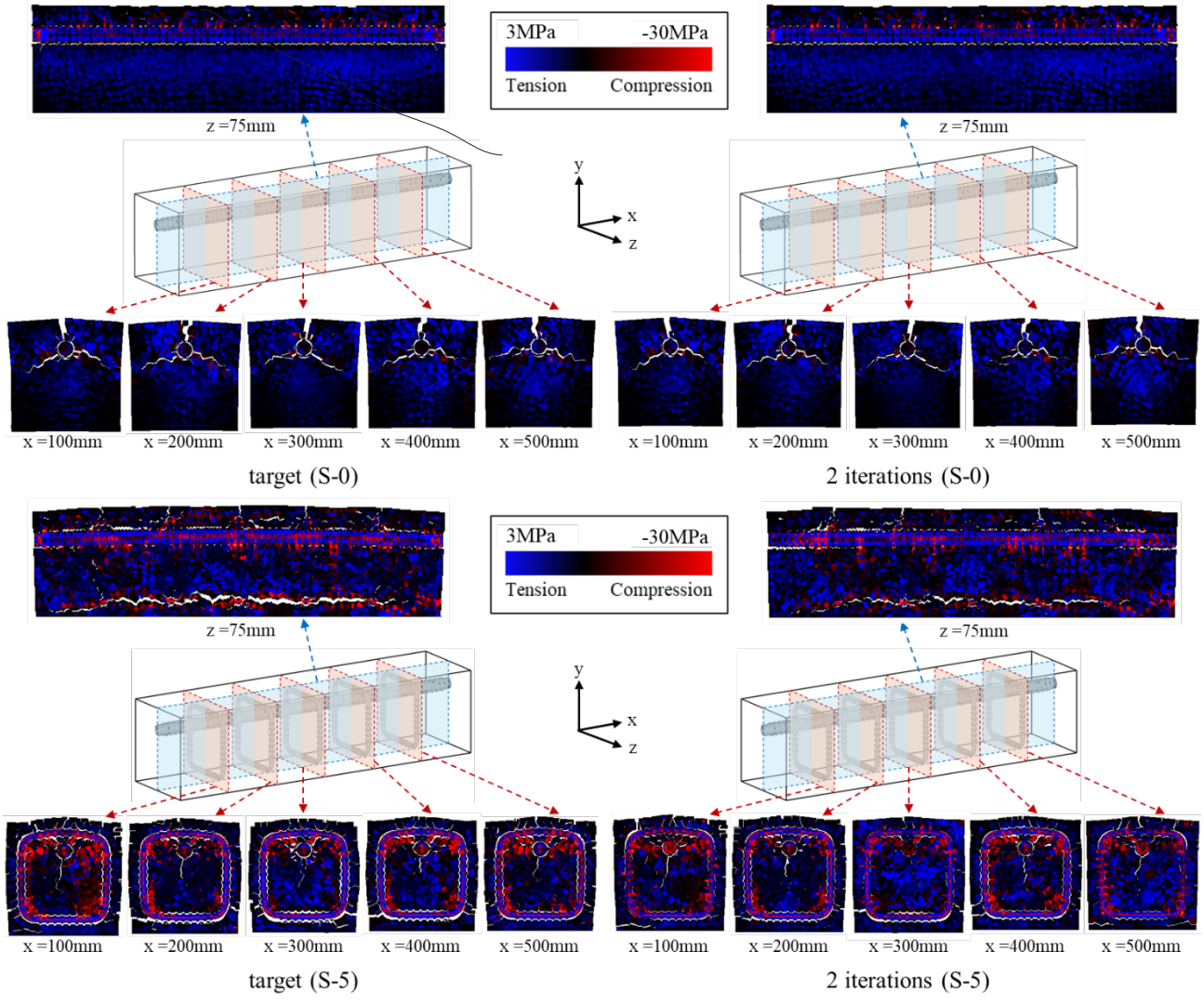

Fig. 11. Internal stress and cracking conditions of target and 2 iterations (deformation magnified 10 times)

accuracy, demonstrating the potential applicability of the proposed approach to more complex estimation problems, such as multi-rebar RC models with intricate stress states.

Acknowledgements

The author acknowledges the organisers of the Asian Concrete Federation 20th Anniversary Workshop (in particular Prof. Caijun Shi, Prof. Zhenguo Shi, and other colleagues at Hunan University, Changsha) for the invitation to participate in this event, and also many colleagues who engaged in thought-provoking conversations during the event itself, which have led directly to the framing of this paper in its current form.

CRediT authorship contribution statement

Keita Tateishi: Conceptualization, Methodology, Writing – original draft.

Tianyu Shao: Conceptualization, Methodology, Writing - review & editing.

Kohei Nagai: Conceptualization, Supervision, Writing – review & editing.

Declaration of competing interest

The authors declare that they have no known competing financial interests or personal relationships that could have appeared to influence the work reported in this paper.

Reference

[1] Raupach, M. (2006) "Models for the propagation phase of reinforcement corrosion – An overview," Materials and Corrosion, 57(8), pp. 605–613, DOI: https://doi.org/10.1002/maco.200603991.

[2] Elsener, B.; Andrade, C.; Gulikers, J.; Polder, R.; and Raupach, M. (2003) "Half-cell poten-tial measurements – Potential mapping on rein-forced concrete structures," Materials and Structures, 36(261), pp. 461–471, DOI: https://doi.org/10.1007/BF02481526.

[3] Azarsa, P.; and Gupta, R. (2017) "Electrical Resistivity of Concrete for Durability Evaluation: A Review," Advances in Materials Science and Engineering, 2017, DOI: https://doi.org/10.1155/2017/8453095.

[4] Pereira, E. V.; Salta, M. M.; and Fonseca, I. T. E. (2015) "On the measurement of the polarisation resistance of reinforcing steel with embedded sensors: A comparative study," Materials and Corrosion, 66(10), pp. 1029–1038, DOI: https://doi.org/10.1002/maco.201407910.

[5] Ohtsu, M.; and Tomoda, Y. (2007) "Corrosion process in reinforced concrete identified by acoustic emission," Materials Transactions, 48(6), pp. 1184–1189, DOI: https://doi.org/10.2320/matertrans.I-MRA2007844.

[6] Verstrynge, E.; Van Steen, C.; Vandecruys, E.; and Wevers, M. (2022) "Steel corrosion damage monitoring in reinforced concrete structures with the acoustic emission technique: A review," Construction and Building Materials, 349, p. 128732, DOI: https://doi.org/10.1016/j.conbuildmat.2022.128732.

[7] Verma, S. K.; Bhadauria, S. S.; and Akhtar, S. (2014) "Monitoring corrosion of steel bars in reinforced concrete structures," The Scientific World Journal, 2014, DOI: https://doi.org/10.1155/2014/957904.

[8] Zhang, M.; Akiyama, M.; Shintani, M.; Xin, J.; and Frangopol, D. M. (2021) "Probabilistic estimation of flexural loading capacity of existing RC structures based on observational corrosion-induced crack width distribution using machine learning," Structure and Infrastructure Engineering, 91, p. 102098, DOI: https://doi.org/10.1016/j.strusafe.2021.102098.

[9] Jiradilok, P.; Nagai, K.; and Matsumoto, K. (2019) "Meso-scale modeling of non-uniformly corroded reinforced concrete using 3D discrete analysis," Engineering Structures, 197, p. 109378, DOI: https://doi.org/10.1016/j.engstruct.2019.109378.

[10] Jiradilok, P.; Wang, Y.; Nagai, K.; and Matsumoto, K. (2020) "Development of discrete meso-scale bond model for corrosion damage at steel–concrete interface based on tests with/without concrete damage," Construction and Building Materials, 236,

p. 117615, DOI: https://doi.org/10.1016/j.conbuildmat.2019.117615.

[11] Avadh, K.; Jiradilok, P.; Bolander, J. E.; and Nagai, K. (2021) "Mesoscale simulation of pull-out performance for corroded reinforcement with stirrup confinement in concrete by 3D RBSM," Cement and Concrete Composites, 116, p. 103895, DOI: https://doi.org/10.1016/j.cemconcomp.2020.103895.

[12] Joshi, S. S.; Avadh, K.; Singh, V.; Jiradilok, P.; and Nagai, K. (2022) "Investigating the effect of rebar corrosion order and arrangement on cracking behaviour of RC panels using 3D discrete analysis," Construction and Building Materials, 325, p. 126730, DOI: https://doi.org/10.1016/j.conbuildmat.2022.126730.

[13] Kuntal, V. S.; Jiradilok, P.; Bolander, J. E.; and Nagai, K. (2021) "Estimation of internal corrosion degree from observed surface cracking of concrete using mesoscale simulation with model predictive control," Computer-Aided Civil and Infrastructure Engineering, 36(5), pp. 544–559, DOI: https://doi.org/10.1111/mice.12620.

[14] Kuntal, V. S.; Jiradilok, P.; Bolander, J. E.; and Nagai, K. (2021) "Estimating corrosion levels along confined steel bars in concrete using surface crack measurements and mesoscale simulations guided by model predictive control," Cement and Concrete Composites, 124, p. 104233, DOI: https://doi.org/10.1016/j.cemconcomp.2021.104233.

[15] Shao, T.; Luo, J.; and Nagai, K. (2025) "Estimating RC corrosion distribution from surface cracks using mesoscale analysis integrated with machine learning," Cement and Concrete Composites, 157, p. 105950, DOI: https://doi.org/10.1016/j.cemconcomp.2025.105950.

[16] Kawai, T. (1978) "New discrete models and their application to seismic response analysis of structures," Nuclear Engineering and Design, 48(1), pp. 207–229, DOI: https://doi.org/10.1016/0029-5493(78)90217-0.

[17] Nagai, K.; Sato, Y.; and Ueda, T. (2005) "Mesoscopic simulation of failure of mortar and concrete by 3D RBSM," Journal of Advanced Concrete Technology, 3(3), pp. 385–402, DOI: https://doi.org/10.3151/jact.3.385.